Epitaxy and electronic structure of $p(1\times1)$ Cr/Au(100)

G. Zajac,* S. D. Bader, and R. J. Friddle

Materials Science and Technology Division, Argonne National Laboratory, Argonne, Illinois 60439

(Received 26 November 1984)

Low-energy electron-diffraction, Auger-electron, He I photoemission, and electron-energy-loss spectroscopies were used to characterize the epitaxy and electronic structure of Cr overlayers deposited on single-crystal Au(100). Epitaxy was achieved for substrate-deposition temperatures above ~100—$150\,°C$. The observed strain-free $p(1\times1)$ Cr/Au(100) epitaxy is due to the fortuitous matchings of the primitive two-dimensional square nets of Cr(100) and Au(100) bulk terminations. Surface states near the Fermi energy of pure Cr(100) are found to persist at the Cr-Au interface, in agreement with recent theoretical findings. The electronic structure of Cr multilayers on Au(100) is closely related to that of ordinary bcc Cr. The results are discussed in terms of the recently reported superconducting behavior of Au/Cr/Au(100) sandwiches attributed to fcc Cr possessing the 41%-expanded lattice constant of Au. An alternate hypothesis for the sandwich superconductivity is suggested in terms of disordered Cr.

I. INTRODUCTION

The fabrication and characterization of metal-on-metal films has generated much recent interest.[1] The reasons are twofold. Firstly, technical advances permit unprecedented control of the growth parameters, to ensure high-quality materials. Secondly, the expectation is that there will be new applications for such advanced materials, as has occurred in the semiconductor field. In the present study we are concerned with the system Cr deposited on Au(100). The epitaxy is expected to be strain free due to the fortuitous matching of the primitive, two-dimensional square nets of Cr(100) and Au(100). The electronic structure is also a topic of much interest. Cr, Mo, and W are all group-VIB transition metals with bcc crystal structures, and with low electronic densities of states at the Fermi energy, $N(E_F)$. It is well known that surface states are prone to emerge where there are gaps in the bulk bands. Specifically, for the cases of Cr(100),[2-5] Mo(100),[6] and W(100),[7] surface states near E_F have been calculated theoretically and are believed to dominate the surface properties. For Mo(100) and W(100) the high density of surface states is believed to drive the observed surface reconstructions. The mechanism involves surface charge-density-wave—driven periodic lattice distortions arising from the nesting of the Fermi surface.[7,8] For Cr(100) there is no such reconstruction, but the most recent photoemission evidence strongly suggests the existence of a magnetic surface layer with an enhanced ordering temperature relative to the bulk Néel temperature.[9]

In the bulk, high values of $N(E_F)$ are known to be associated not exclusively with charge-density-wave or magnetic instabilities, but also with superconductivity. From this vantage point the Cr-on-Au(100) system is again of particular interest. Brodsky *et al.*[10,11] have recently reported superconductivity in (~25 Å thick) multilayers of Cr sandwiched between thick Au(100) films. The question arises as to whether Cr surface states can be implicated here; but first it must be ascertained whether the pure Cr(100) surface states can persist at the Cr-Au interface. In this regard it is of interest that Feibelman and Hamann[4] have recently self-consistently calculated the electronic properties of clean Cr(100) and Cr(100) covered with a monolayer (ML) of Au(100). They concluded that Cr surface states near E_F do indeed persist at the metal-metal interface.

The dilemma is that, ordinarily, a high $N(E_F)$ value might be expected to be associated with either magnetism *or* superconductivity, but not with both. Brodsky *et al.*[10,11] advanced a hypothesis that circumvented this problem. They attributed the superconductivity to a new fcc phase of Cr that possesses the Au lattice constant. In this hypothesis the surface properties of bcc Cr and the bulk antiferromagnetism are irrelevant. The fcc phase *is* expected to possess the requisite high value of $N(E_F)$.[12] Supporting evidence for fcc Cr comes from synchrotron x-ray-diffraction experiments recently performed on Au/Cr/Au(100) sandwiches.[13] Weak satellites straddling the Au[200] reflection were attributed to a thin fcc layer. Anomalous scattering experiments confirmed the participation of Cr in producing the satellites.[13] However, in the same study, extended x-ray-absorption fine structure (EXAFS) was observed to be identical to that from a bcc Cr standard. The conclusion was that the sandwich was, at best, mixed-phase fcc-bcc Cr.

The purpose of the present study was to explore the epitaxy and electronic structure of the Cr-Au(100) interface by means of *in situ* electron spectroscopic and surface investigations, and to attempt to relate the findings to the intriguing surface magnetism and superconductivity studies cited above. The outline of the remainder of the paper is as follows: Section II contains experimental details. Sections III A—III D contain low-energy electron-diffraction (LEED), Auger-electron, photoemission, and electron-energy-loss results, respectively. Section IV contains a discussion of the relationship of the present results to previous findings. New hypotheses are proposed to reconcile aspects of the rather disparate studies. Finally, the highlights are briefly summarized in Sec. V.

II. EXPERIMENTAL PROCEDURES

The experiments were performed in a stainless-steel chamber equipped with a Physical Electronics double-pass cylindrical mirror analyzer (CMA) with a coaxial electron gun, a Varian Associates LEED system, and a VG ultraviolet lamp. The base pressure was in the mid-10^{-11}-Torr range, and was maintained with ion, titanium-sublimation, and turbomolecular pumps. Data were collected with the aid of a laboratory microcomputer and stored on disk, as described previously.[14]

A Cr evaporator was constructed by mounting high-purity Cr foil onto a Ta backing sheet (~ 0.005 in. thick). The sheet was mounted on a $2\frac{3}{4}$-in. Conflat flange via two high-current copper electrical feedthroughs. The entire assembly was physically shielded by a cylindrical Ta can with an evaporation aperture of dimensions 3×6 mm. A typical evaporation rate of $\sim \frac{1}{6}$ Å/min could be achieved at a Cr foil temperature of ~ 800 °C. Previously, we used a similarly styled Cu evaporator in Cu/Ru(0001) studies.[15]

The Au(100) single crystal was $5 \times 10 \times 1$ mm in size. It was oriented, cut, and polished in a standard manner to within 1° of the proper orientation. Mechanical polishing down to 0.05 μm using Buehler diamond grit on a vibratory wheel was followed by electropolishing in an HCl-ethanol-glycerine solution. The Au(100) was cleaned by sputter-anneal cycles at Ar$^+$-ion beam energies of ~ 500 eV. The sample heater was a resistive button to which the sample was mounted. The Au could be heated to 800 °C, but was more typically flash-cleaned at 600 °C and annealed at ~ 100 °C. The cleanliness of the sample was carefully monitored via Auger-electron spectroscopy throughout the course of the experiments.

III. RESULTS

A. Low-energy electron diffraction

The clean Au(100) gave the distinctive (5×20) LEED pattern expected for the clean, reconstructed surface. While it is known that oxygen bombardment could be used to yield an unreconstructed $p(1 \times 1)$ surface structure,[16] it was found that small doses of Cr ($\gtrsim 5\%$ of a monolayer) more conveniently reverted the Au(100) surface to its unreconstructed form. Cr could then be removed from the Au(100) surface by heating to temperatures $\gtrsim 550$ °C. This is supported by the disappearance of the Cr 529-eV Auger-electron-spectroscopy (AES) signal, and the reappearance of the (5×20) LEED pattern of clean, reconstructed Au(100). It is known that small amounts of adsorbed gases can also revert the (5×20) to the $p(1 \times 1)$ Au(100) structure. Thus, there appears to be a delicate energetic balance between (1×1) and (5×20) Au(100). This is in contrast to the high stability of many semiconductor reconstructions.

Upon Cr deposition at Au substrate temperatures above $\sim 100-150$ °C, a sharp $p(1 \times 1)$ LEED pattern persisted to the highest dosages studied (~ 15-ML equivalents). This, along with the AES data to be introduced in Sec. III B, confirms the strain-free epitaxy expected for Cr/Au(100) based on the registry of the Cr(100) and

Au(100) bulk terminations. The fcc Au bulk lattice constant is 4.08 Å. The primitive square-net lattice constant of the Au(100) surface is $4.08/\sqrt{2} = 2.88$ Å. The bcc Cr bulk lattice constant and primitive (100)-face square-net lattice constant are also both 2.88 Å. For substrate temperatures above 500–550 °C, Cr evaporated from (and probably also dissolved into) the Au. For room temperature substrate depositions the LEED pattern would progressively become diffuse, indicative of disordered Cr overlayers. This observation will play a role in the superconductivity discussion of Sec. IV. Subsequent annealing of such disordered surfaces above $\sim 100-150$ °C would order the Cr overlayers to the sharp $p(1 \times 1)$ structure.

A simple kinematic approach was taken in an attempt to elucidate the fcc versus bcc Cr question. An ordered Cr multilayer was deposited on the Au(100) surface to a thickness sufficient to totally attenuate the Au LEED beams. An (00)-beam intensity-versus-energy profile was obtained close to normal incidence ($\theta \cong 11°$). In this geometry kinematic peaks would be associated with (00l) reflections, where l is an even integer. The diffraction condition is $l\lambda = 2d \cos\theta$, where d is the interlayer repeat distance, and the incident-electron wavelength λ is pro-
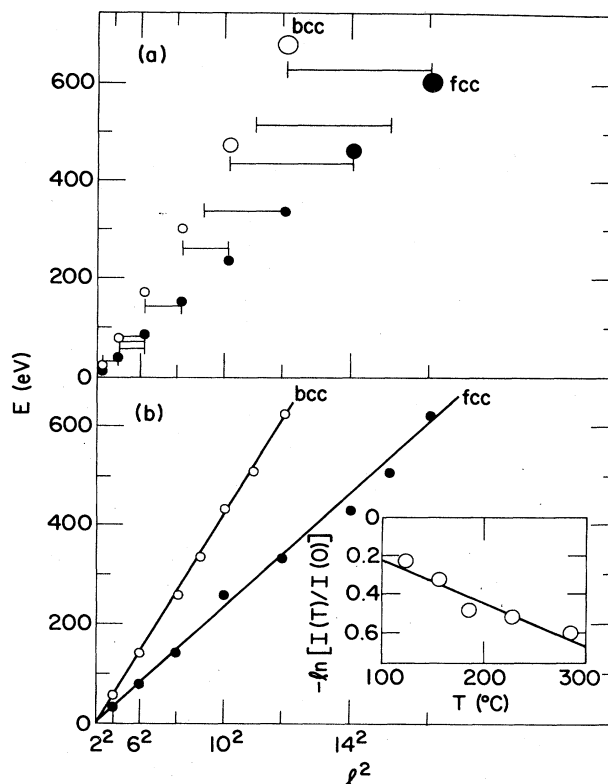

FIG. 1. Kinematic analysis of specular LEED beam. Panel (a) shows the energies of the expected (00l) reflections for bcc ($\bigcirc$) and fcc ($\bullet$) d spacings with $U = 0$. The horizontal lines are the energies of measured reflections, and the small vertical marks on these lines indicate the assigned l indices. The two sets of indexed data appear again in panel (b), along with straight-line fits that yield the d and U values that appear in Table I. The inset of panel (b) is a Debye-Waller plot for the 144-eV reflection that yields $\Theta_D = 450$ K.

portional to $(E-U)^{-1/2}$, where E is the energy of the diffraction peak and U is the inner potential for Cr. A plot of E versus l^2 should then produce a straight line whose slope yields d, and whose $l=0$ intercept yields U, since $E-U \propto (d\cos\theta)^{-2}l^2$. This approach has been successfully used to obtain d spacings in agreement with the known bulk values to the few percent level for Cu(100) and Ni(100),[17] Pd(100),[18] and Cr(110).[19] Thus, it seemed that with a 41% difference between $d_{bcc}=2.88$ Å and $d_{fcc}=4.08$ Å, an unambiguous answer should be possible.

In the present case difficulty arises in indexing the reflections. The method used is outlined in Fig. 1. Figure 1(a) shows E versus l^2 calculated at even-l values using d_{bcc} (open circles) and d_{fcc} (solid circles) with $U=0$. The horizontal bars are the experimental energies at which diffraction peaks occurred. Indexing was accomplished by assigning the bcc or the fcc l value that most closely intersects each horizontal bar in the vicinity of the calculated lines. These intersections are denoted by the short vertical lines on the horizontal bars in Fig. 1(a), and are reproduced as circles in Fig. 1(b). (Note that some odd-l forbidden reflections are observed, due to surface sensitivity.) The straight lines in Fig. 1(b) were obtained by the linear least squares method. Table I summarizes the derived d and U values. Unfortunately it is found that the data can be bcc or fcc indexed. In both cases Table I shows that agreement with bulk d spacings to the few percent level is obtained, and also that the inner potential values are not unreasonable. The quality of the fits as judged by the rms deviations tend to favor the bcc choice, as does agreement with the reported U value[19] for Cr(110), -16 eV. However, the numerous simplifying assumptions inherent in the methodology may raise questions about such close scrutinization of the results.

One final LEED experiment was performed in another attempt to apply kinematic analysis to differentiate between fcc and bcc Cr. Since the fcc interlayer spacing is 41% dilated compared to the corresponding bcc Cr d spacing, it is reasonable to assume that the average fcc interlayer force constant is weaker than that for the bcc structure. This quantity is accessible via a Debye-Waller analysis of the reflections studied in Fig. 1. To quantify the expectation we take the standard value for the lattice Grüneisen constant, $\Gamma \equiv -(\partial \ln\Theta_D/\partial \ln V)=2$, where Θ_D is the Debye temperature and V is the volume. For an $\sim 40\%$ increase in V, an $\sim 80\%$ decrease in Θ_D would then be predicted. The bulk[20] Θ_D for bcc Cr is 600 K; thus, a corresponding value for fcc Cr would be near room temperature. Surface values for Θ_D deduced from LEED studies are generally significantly lower than bulk values. The inset of Fig. 1(b) shows a Debye-Waller plot for 144-eV Cr(00l) reflection. The slope yields a Θ_D value

TABLE I. Bulk d spacings compared to fit parameters extracted from Fig. 1(b) for fcc and bcc Cr.

	d_{bulk} (Å)	d_{fit} (Å)	U (eV)
fcc[a]	4.08	4.04	-5.2
bcc	2.88	2.94	-16.8

[a]Hypothesized.

of 450 K. This value is well above that estimated above for fcc Cr, but is quite reasonable for bcc Cr. We take this to support a bcc Cr identification, although we recognize the indirectness of the evidence. Support for the bcc identification from photoemission experiments appears in Sec. III C, but first the Auger results will be presented.

B. Auger-electron spectroscopy

Auger-electron spectroscopy was used to (i) monitor the purity of the surface under study, (ii) calibrate the evaporator, and (iii) study the growth mechanism of Cr on Au(100). Previous experiences with bulk crystals of Cr, V, and Ti provided us with confidence that reactive surfaces could be properly preserved in our ultrahigh-vacuum (UHV) chamber.[21] The contaminants S, C, and O were always below the 1–2% coverage level on the surface. Nitrogen contamination was not observed, although it can be a problem for bulk Cr crystals.

To calibrate the evaporator, Cr and Au AES signals were monitored as a function of deposition time. This required rotating the sample manipulator between the evaporator and CMA ports of the UHV chamber. Figure 2 shows the peak-to-peak heights versus deposition time of the Au 69-eV and Cr 529-eV AES signals. The data were obtained from scans between 20 and 1020 eV, so all relevant Auger transitions were monitored. The evaporator was operated at the same constant current during all depositions to assure a constant flux, as in earlier Cu/Ru(0001) studies.[15] In Fig. 2 there is a change in slope at ~ 6–8 min, after an initially linear buildup of Cr signal. This is interpreted as the completion point for the formation of a monolayer of Cr. The slope change reflects the surface sensitivity of the Auger electrons and the self-attenuation of signal that results. The Au signal in Fig. 2 mirrors the Cr trend. There is an initially linear decrease of Au signal and a break in slope at the same point in time as for Cr. Figure 2 indicates that the Cr covers the Au. The breakpoint serves as the working definition for a monolayer of Cr deposited. Evaporation time then converts to monolayer equivalents of Cr. The AES calibration procedure was performed at various stages
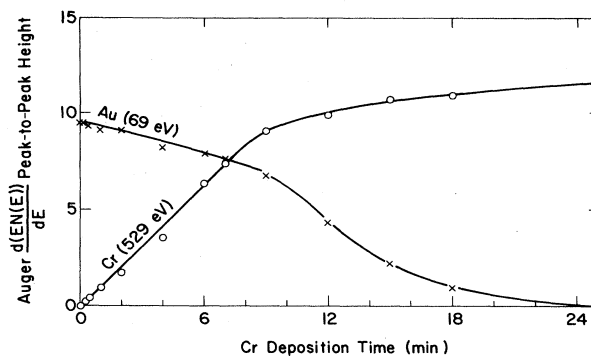

FIG. 2. Auger signals for Au and Cr vs Cr deposition time. The break in slope from initially constant values defines the completion of the first Cr monolayer. The increased rate of attenuation of the Au signal beyond the monolayer stage is not well understood.

throughout the study and found to be highly reproducible.

Both the Frank—van der Merwe (FvdM) and the Stranski-Krastanov (SK) film-growth mechanisms begin with the formation of an epitaxial monolayer. The difference between the two mechanisms is that in the former growth continues in a layer-by-layer manner, while in the latter island growth ensures.[22] In the FvdM mechanism, slope changes in Fig. 2 are predicted to occur at uniform intervals in time, indicative of the formation of successive monolayers. Such behavior is not observed in Fig. 2. Most likely that is due to limited experimental sensitivity to successively smaller slope changes. There is, however, reason to favor the FvdM over the SK mechanism. This is based on the results of the photoemission, energy-loss, and LEED intensity-energy scans. These experiments indicate a rapid attenuation of Au-derived features at the few monolayer stage. In SK growth such features would have been expected to persist well beyond this stage, since there would be only thin overlayers attenuating the Au signal from between Cr islands.

C. Ultraviolet photoelectron spectroscopy

The ultraviolet-photoelectron-spectroscopy results provide information on (i) the work-function change with Cr coverage, (ii) the interaction of the Au and Cr d bands, and (iii) the evolution of the Cr d band. The work func-

tions of Au(100) (Ref. 23) and Cr(100) (Ref. 24) are known to be 5.47 and 4.46 eV, respectively. Upon Cr deposition the work function was observed to rapidly drop by 0.6 eV by ~0.2 ML (see inset in Fig. 3). Further deposition left the work function unchanged beyond this value. No evidence was found for an oscillatory work-function change with coverage, in agreement with the calculations of Feibelman and Hamann.[4]

The He I ultraviolet-photoelectron-spectroscopy (UPS) results ($h\nu=21.2$ eV) are shown in Fig. 3. Note that the pure-Au spectrum is in good agreement with previous experimental results[25] and bulk band calculations.[26] The prominence of the feature at the bottom of the Au d band has been attributed to a final-state band-structure enhancement at this photon energy.[25] Figure 3 shows the results for submonolayer, monolayer, and multilayer Cr depositions. The bottom of the Cr d band and the top of the Au d band appear to hybridize. The changes in the top of the Au d band can also be attributed to removal of Au surface states. No surface band-structure calculations, however, are presently available for Au(100) to check the location of surface states. The Au d—band features are observed to attenuate rapidly with Cr dosage, indicative of an abrupt Au-Cr interface, as was emphasized previously.

In Fig. 4 the data for the first 2 eV of the binding energy (BE) are replotted from Fig. 3 to emphasize the Cr d—band evolution. The peak heights for submonolayer, monolayer, and multilayer Cr dosages are normalized to each other. Focusing first on the multilayer spectrum, two features are clearly observed: a broad peak at 1 eV
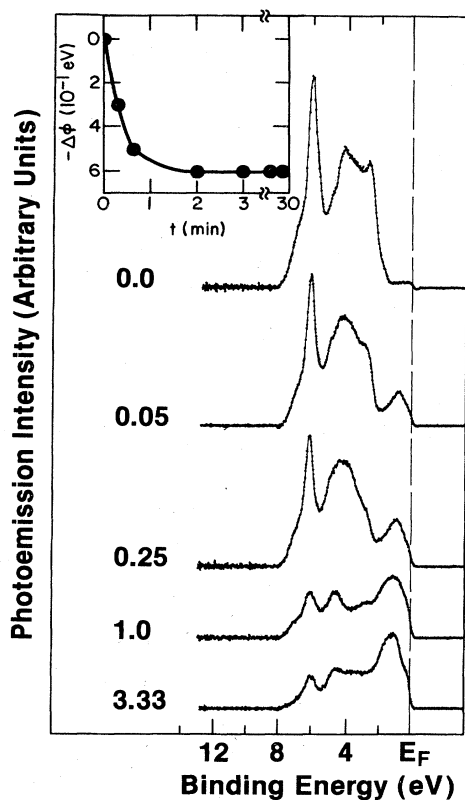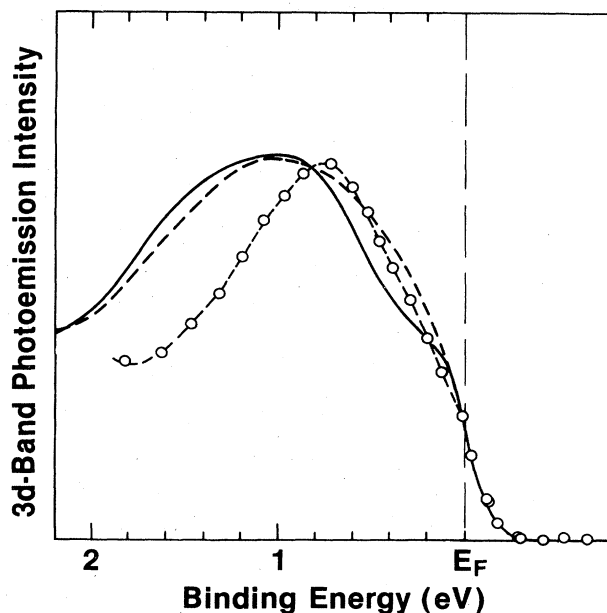

FIG. 3. He I photoemission results ($h\nu=21.2$ eV). The Cr doses are indicated to the left of each spectrum in monolayer equivalents. Smooth secondary-electron backgrounds were subtracted from each spectrum for clarity. The inset shows the work-function decrease as a function of Cr deposition time.

FIG. 4. He I photoemission study of the Cr d—band evolution. The spectra are normalized to each other at the peak intensity. The solid curve is for the multilayer, the dashed curve is for the monolayer, and the circle-dash curve is for the dilute submonolayer Cr spectrum of Fig. 3. Note that the broad peak at 1 eV BE and shoulder at ~0.1 eV BE for the multilayer spectrum are very similar to the surface-state features observed on clean Cr(100).

BE and a shoulder near 0.1 eV BE. The most striking aspect of this spectrum is its relationship to that reported for pure Cr(100) by Klebanoff et al.[9] The bulk density of states of Cr has its d-band peaks removed to higher BE.[27] Both of these features are identified as surface states. The pure-Cr(100) spectrum of Ref. 9 was taken with an angle-resolved spectrometer at normal emission. The dominant peak was 0.8 eV and the minor feature was at 0.15 eV. In a separate angle-resolved experiment in normal emission at the Synchrotron Radiation Center, Stoughton, Wisconsin, we observed identical binding energies for 1–2 ML Cr on Au(100).[28] We interpret the agreement between pure-Cr(100) and Cr/Au(100) photoemission features to indicate the presence of a bcc-like surface-electronic structure for the epitaxial film. In the study of Klebanoff et al.,[9] evidence was found for a magnetic surface layer of Cr with an enhancement ordering temperature relative to the Néel temperature of bulk bcc Cr, as was mentioned in the Introduction.[29] From this perspective we would interpret the small changes observed in Fig. 4 for monolayer and submonolayer Cr relative to multilayer Cr as arising from changes in the exchange splittings with geometry. The spectra can clearly be derived from each other.

D. Electron-energy-loss spectroscopy

Electron-energy-loss spectroscopy (EELS) provides information on the collective plasma excitations, and on the core-level transitions. The question is to what extend does the excitation spectrum of Cr epitaxially deposited on Au(100) resemble that of pure bcc Cr? Fortunately, we recently completed a study[21] of the $3p$-to-$3d$ transitions of pure Cr, so we are in a particularly favorable position to make such a comparison. Figure 5(a) shows broad-scan loss spectra that include plasmon and core-level excitations for pure Au(100) and Cr-dosed Au(100) up to the thick multilayer regime. Figure 5(b) shows narrower scans of the core-level loss region. A point to emphasize in Fig. 5(a) is that the pure-Au(100) features rapidly attenuate with Cr dosage, again indicative that Cr forms uniform overlayers covering the Au. Upon going from pure Au(100) to multilayer Cr(100), the plasmon features change in energy from those published[30] for Au to those published[31] for Cr. In Fig. 5(b) an actual comparison is made to our earlier spectrum[21] of the $3p$-to-$3d$ transitions for pure Cr. The multilayer Cr-on-Au(100) spectrum is identical in appearance to that for bcc Cr. These comparisons serve as further verification that the electronic signature of Cr on Au(100) is bcc Cr–like.

For thin Cr overlayers there appears to be a significant spectral change in Fig. 5(b), in that a 61-eV feature appears where there was a 57-eV feature for the multilayer Cr. However, the 61-eV feature is identified as the $5p_{3/2}$ (O_3) resonance of Au, based on comparison with the definitive Au EELS study of Dietz et al.[32] Careful examination of Fig. 5 supports this in that the 61-eV feature is most intense for the pure-Au spectrum. Also, Dietz et al.[32] observed that the $5p_{3/2}$ resonance far outweighed in intensity the neighboring $5p_{1/2}$ (O_2) and $4f$ ($N_{6,7}$) excitations of Au, which are not apparent in Fig. 5.
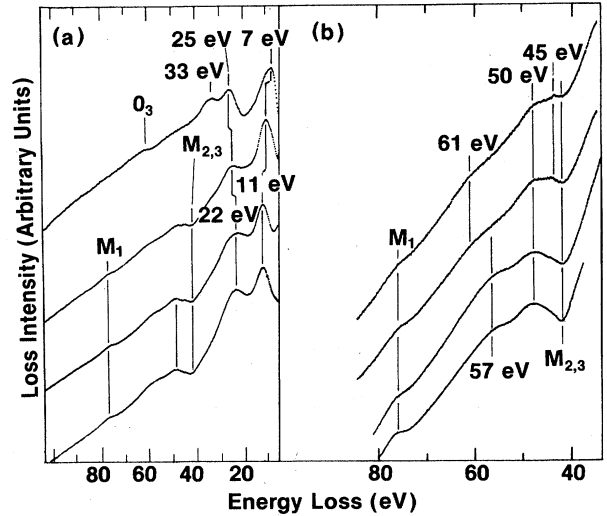

FIG. 5. Electron-energy-loss spectra are shown in panel (a) for (top to bottom) clean (5×20) Au(100), 1.7, 3.3, and 15 ML Cr, and panel (b) for (top to bottom) 1.7, 3.3, and 15 ML and bulk Cr. In panel (a) the plasma-type loss of Au at 7 eV evolves into the 11-eV loss of Cr, that at 25 eV evolves into the 22-eV Cr loss, and that at 33 eV rapidly attenuates with Cr deposition. The core-level losses are expanded in panel (b). The Cr $M_{2,3}$ resonance has identical minima at threshold (43 eV) and peaks at 50 and 57 eV for multilayers Cr/Au(100) and bcc Cr(100). The thin Cr/Au(100) samples show an interesting near-threshold feature at 45 eV as well. The weaker Cr M_1 and Au O_3 (61 eV) losses are also identified. The primary beam energy is 200 eV.

IV. DISCUSSION

A prime motivation of the present study was to elucidate the superconductivity of Au/Cr/Au(100) sandwich structures reported in Refs. 10 and 11. The hypothesis adopted in that study was that the Cr became fcc with the Au lattice constant. This would require a most unusual volume increase of 41%, which should certainly be accomplished by a dramatic rearrangement of the electronic structure. However, the present results all seem compatible with a bcc-like electronic structure, including the LEED-derived inner potential value, Debye temperature, and kinematic beam indexing, the work function, the spectral loss features, and, most importantly, the photoemission-derived surface states. These latter results, when compared to the pure-Cr(100) study of Klebanoff et al.,[9] are suggestive of magnetic interactions at the surface as well, and would thus tend to preclude superconductivity.

We explore alternate hypotheses to account for the superconducting sandwich behavior. The fcc model had the advantage of providing the high value of $N(E_F)$ necessary for superconductivity.[12] Another way to increase the $N(E_F)$ of Cr would be to make it amorphous or highly disordered.[33] The band structure would then smear out, $N(E_F)$ would increase, and peaks in $N(E)$ would decrease in height. Note that the sandwich structures reported in

Refs. 10 and 11 were deposited on room-temperature substrates. We observed disordered LEED patterns for Cr depositions at substrate temperatures below $\sim 100\,°C$, while epitaxy occurred above $\sim 100-150\,°C$. Recent unpublished results[34] for four Au/Cr/Au(100) sandwiches grown at 130 °C indicated a lack of superconductivity (to 0.4 K), while previous sandwich structures had ordering temperatures T_c in excess of 2 K. If the disorder hypothesis is correct, superconductivity should occur in sandwiches fabricated from low-temperature (LN$_2$) depositions.[33] This needs to be tested. Extension of the disorder hypothesis to the *depressed* T_c values reported[11] for Au/V/Au(100) sandwiches is natural, since it is known[35] that amorphous V has a lower T_c than crystalline V. Superconductivity has been reported for Cr thin films deposited by noble-gas ion-beam—sputtering techniques.[36] T_c values up to 1.5 K were reported and associated with bcc-lattice-constant dilations of only 3%, attributed to the formation of dilute noble-gas solutions.

Another way to increase $N(E_F)$ at the interface is to have charge transfer between Au and Cr. Since $N(E_F)$ for bulk Cr is at a minimum between two peaks, $N(E_F)$ would increase irrespective of the direction of charge transfer. The problem with this idea is that order versus disorder would not affect the superconductivity. However, as cited above,[34] it was observed that superconductivity did disappear when growth conditions favored epitaxy.

Finally, the surface states themselves provide a high value of $N(E_F)$ at the interface. The expectation, however, is that these surface states are magnetic,[9] not superconducting. Otherwise there would be some appealing features present. In thin films the effect of proximity of the superconductor to the normal metal degrades T_c.[37] This is because the attractive interaction between electrons is weakened when the Cooper pairs tunnel into the normal metal. The localization of the surface states near E_F would tend to prevent the Cooper pairs from entering the normal metal.[4] The proximity effect then would not have a pronounced affect on T_c.[4]

For superconductivity attributable to fcc Cr with the Au lattice constant, the idea of p-wave pairing[38] is evoked. This is because the dramatic fcc volume increase would tend to localize the itinerant-d-electron magnetism of bcc Cr. Such p-wave speculation might as plausibly apply to superconducting surface states of bcc Cr, due to their presumed magnetic character. However, even Ce, which has a large (16%) volume change and electronic

transformation at the γ-α phase transition, does not become superconducting until it is in the high-pressure α' phase.[39] It can also be argued that the 41% volume increase necessary for the existence of the fcc Cr is intuitively unrealistic to expect. Recent total-energy calculations[40] as a function of lattice constant for fcc Cr and Cr-Au(100) superlattice geometries fail to justify Cr expansion to the Au lattice spacing. The question then would be can the synchrotron x-ray-diffraction experiment of Ref. 13 be reinterpreted? For instance, would Cr substitutionally replacing Au atoms in the fcc Au lattice give an fcc Cr signature?

V. SUMMARY

The Cr-on-Au(100) system was studied to obtain insight into the reported superconductivity of Au/Cr/Ar(100) sandwiches, attributed to fcc Cr with the Au lattice constant.[10,11] Our LEED, and photoemission and loss spectroscopy, results, taken together, are readily consistent with a bcc model for the Cr structure. This is supported by EXAFS experiments[13] and recent total-energy calculations,[40] but is in contrast to a novel synchrotron x-ray-diffraction experiment.[13] We attribute the superconductivity of the sandwiches to disordered Cr. Our LEED results support the disorder hypothesis since epitaxy required substrate temperatures above $\sim 100-150\,°C$, while the superconducting sandwiches of Refs. 10 and 11 were prepared at room temperature.

The surface states of Cr near E_F, observed[9] and calculated[2-5] for pure Cr(100), and believed to be magnetic in origin, are preserved at the Cr/Au(100) interface. This is of interest in itself, since surface states are usually very sensitive to changes in environment. Similar conclusions were drawn from Au/Cr(100) self-consistent band-structure calculations of Feibelman and Hamann.[4] The ability to realize strain-free epitaxy on a metal-on-metal system, the apparent abruptness of the interface, and the prominent surface and interfacial states near E_F make the Cr/Au(100) system particularly challenging to study further.

ACKNOWLEDGMENTS

*Present address: Amoco Research Center, P.O. Box 400, Naperville, IL 60566.

[1]For references, see, for instance, Pei-Lin Cao, D. E. Ellis, A. J. Freeman, Quing-Qi Zheng, and S. D. Bader, Phys. Rev. B. 30, 4146 (1984).

[2]G. Allan, Surf. Sci. 74, 79 (1978); Phys. Rev. B 19, 4774 (1979).

[3]D. R. Grempel, Phys. Rev. B 24, 3928 (1981).

[4]P. J. Feibelman and D. R. Hamann, Phys. Rev. B 29, 6463 (1984); 31, 1154 (1985).

[5]C. L. Fu and A. J. Freeman (unpublished).

[6]G. P. Kerker, K. M. Ho, and M. L. Cohen, Phys. Rev. Lett. 40, 1593 (1978).

[7]M. Posternak, H. Krakauer, A. J. Freeman, and D. D. Koelling, Phys. Rev. B 21, 5601 (1980); H. Krakauer, M. Posternak, and A. J. Freeman, Phys. Lett. 43, 1885 (1979).

[8]E. Tosatti, Solid State Commun. 25, 637 (1978).

[9]L. E. Klebanoff, S. W. Robey, G. Liu, and D. A. Shirley, Phys. Rev. B 30, 1048 (1984).

[10]M. B. Brodsky, P. Marikar, R. J. Friddle, L. Singer, and C. H. Sowers, Solid State Commun. 42, 675 (1982).

[11]M. B. Brodsky and H. C. Hamaker, in *Superconductivity in d- and f-Band Metals 1982*, edited by W. Buckel and W. Weber (Kernforschungszentrum Karlsruhe, Karlsruhe, FRG, 1982), p. 291; M. B. Brodsky, J. Phys. (Paris) Colloq. 45, C5-349

(1984).

[12]Jian-hua Xu, A. J. Freeman, T. Jarlborg, and M. B. Brodsky, Phys. Rev. B **29**, 1250 (1984).

[13]S. M. Durbin, L. E. Berman, B. W. Batterman, M. B. Brodsky, and H. C. Hamaker (unpublished).

[14]G. Zajac, J. Zak, and S. D. Bader, Phys. Rev. B **27**, 6649 (1983); H. C. Hamaker, G. Zajac, and S. D. Bader, *ibid.* **27**, 6713 (1983).

[15]S. D. Bader, L. Richter, P.-L. Cao, D. E. Ellis, and A. J. Freeman, J. Vac. Sci. Technol. A **1**, 1185 (1983); L. Richter, S. D. Bader, and M. B. Brodsky, *ibid.* **18**, 578 (1981).

[16]J. F. Wendelken and D. M. Zehner, Surf. Sci. **71**, 178 (1978); K. H. Reider, T. Engel, R. H. Swendsen, and M. Mannimen, *ibid.* **127**, 223 (1983).

[17]S. Andersson, in *Surface Science* (International Atomic Energy Agency, Vienna, 1975), Vol. 1, p. 77.

[18]S. D. Bader, Surf. Sci. **99**, 392 (1980).

[19]R. Kaplan and G. A. Somorjai, Solid State Commun. **9**, 505 (1971).

[20]N. M. Wolcott, Bull. Inst. Intern. Froid. **1**, 286 (1956); N. Pessall, K. P. Gupta, C. H. Cheng, and P. A. Beck, J. Phys. Chem. Solids **25**, 993 (1964).

[21]S. D. Bader, G. Zajac, and J. Zak, Phys. Rev. Lett. **50**, 1211 (1983); G. Zajac, S. D. Bader, A. J. Arko, and J. Zak, Phys. Rev. B **29**, 5491 (1984).

[22]See, for instance, C. Argile and G. E. Rhead, J. Phys. C **7**, L261 (1974); Surf. Sci. **53**, 659 (1975).

[23]H. B. Michaelson, J. Appl. Phys. **48**, 4729 (1977).

[24]R. J. Wilson and A. P. Mills, Jr., Surf. Sci. **128**, 70 (1983).

[25]K. A. Mills, R. F. Davis, S. D. Kevan, G. Thorton, and D. A. Shirley, Phys. Rev. B **22**, 581 (1980).

[26]A. H. MacDonald, J. M. Daams, S. H. Vosko, and D. D. Koelling, Phys. Rev. B **25**, 713 (1982).

[27]See, for example, V. L. Moruzzi, J. F. Janak, and A. R. Williams, *Calculated Electronic Properties of Metals* (Pergamon, New York, 1978), p. 77; G. Gewinner, J. C. Peruchetti, A. Jaéglé, and R. Pinchaux, Phys. Rev. B **27**, 3358 (1983).

[28]A. J. Arko, G. Zajec, and S. D. Bader (unpublished).

[29]Also see F. Meier, D. Pescia, and T. Schriber, Phys. Rev. Lett. **48**, 645 (1982); G. Rau and S. Eichner, *ibid.* **47**, 939 (1981).

[30]P. Légaré, L. Hilaire, M. Sotto, and G. Maire, Surf. Sci. **91**, 175 (1980).

[31]H. Kato, Y. Sakisaka, M. Nishijima, and M. Ohchi, Surf. Sci. **107**, 20 (1981).

[32]R. E. Dietz, E. G. McRae, and J. H. Weaver, Phys. Rev. B **21**, 2229 (1980).

[33]M. Strongin, in *Superconductivity in d- and f-Band Metals*, edited by D. H. Douglass (AIP, New York, 1972). p. 223; also see M. M. Collver and R. H. Hammond, Phys. Rev. Lett. **30**, 92 (1973).

[34]L. Sill, M. B. Brodsky, and C. H. Sowers (unpublished).

[35]V. M. Kuz'menko, V. G. Lazarev, V. I. Mel'nikov, and A. I. Sudovtsov, Zh. Eksp. Teor. Fiz. **67**, 801 (1974) [Sov. Phys.—JETP **40**, 396 (1975)].

[36]P. H. Schmidt, R. N. Castellano, H. Barz, B. T. Matthias, J. G. Huber, and W. A. Fertig, Phys. Lett. **41A**, 367 (1972); P. H. Schmidt, R. N. Castellano, H. Barz, A. S. Cooper, and E. G. Spencer, J. Appl. Phys. **44**, 1833 (1973); P. H. Schmidt, J. vac. Sci. Technol. **10**, 611 (1973).

[37]W. L. McMillian, Phys. Rev. **175**, 537 (1968).

[38]M. R. Beasley and T. H. Geballe, Physics Today **37**(10), 60 (1984).

[39]J. Wittig, Phys. Rev. Lett. **21**, 1250 (1968).

[40]C. L. Fu, A. J. Freeman, and T. Oguchi (unpublished).